



# Shear response of grain boundary bicrystals with a stacking fault tetrahedron



Lianping Wu, Wenshan Yu\*, Shuling Hu, Shengping Shen\*

State Key Laboratory for Strength and Vibration of Mechanical Structures, Shaanxi Engineering Laboratory for Vibration Control of Aerospace Structures, School of Aerospace, Xi'an Jiaotong University, Xi'an 710049, People's Republic of China

## ARTICLE INFO

### Article history:

Received 22 October 2017

Received in revised form 8 January 2018

Accepted 3 February 2018

### Keywords:

Stacking fault tetrahedron

Grain boundary

Deformation modes

Bicrystal

## ABSTRACT

Stacking fault tetrahedrons (SFTs) are commonly seen in the polycrystalline and nanocrystalline materials due to the heavy plastic deformation, quenching and irradiation. In this study, we present the transformation of SFT near four Cu symmetric tilt grain boundaries (GBs) under shear. Atomistic structures involved in GB deformation and SFT configuration evolutions during the shear are analyzed. Our results show that the presence of SFT has small influence on critical stress corresponding to the incipient plasticity of GB bicrystal. Because GB deformation such as migration, sliding and structure involvement occur at a smaller external shear stress not large enough to activate the destroy of SFT, and SFT near four GBs transforms only when interacting with partial dislocation or GB. Besides, the presence of an SFT does not substantially change the deformation modes of these four GBs. Of one particular case is GB deforming in the complex mechanism due to atom-shuffling, partial dislocation nucleation and local GB dissociations. Significant stress concentration arises around GB due to SFT, which may change the nucleation site of partial dislocations.

© 2018 Elsevier B.V. All rights reserved.

## 1. Introduction

Grain boundaries (GBs) have been widely studied against a background of radiation damage for their potential use as sinks to alleviate radiation damage accumulation [1,2]. During the radiation, quenching and heavy plastic deformation, stacking fault tetrahedrons (SFTs) are observed near GBs in face-centered cubic (fcc) metals with low stacking fault (SF) energy [3]. SFTs, a dominant type of vacancy cluster, present an obstacle for dislocation motion [4,5]. Thus, the presence of SFTs in materials usually causes hardening, embrittlement and plastic instabilities of metal materials [6–9].

Until now, extensive studies of SFT have been carried out and are focused on two aspects. One is the formation mechanisms of SFT (vacancy-originated SFTs and dislocation-based SFTs) [10–12]. The other one is the interaction mechanisms of SFT with different types of defects. Although the structure of SFT is highly stable, SFT is likely to move and its mobility has found to be dependent on its size as well as temperature [13,14]. Based on this, the interactions of SFT with other defects can be divided into two types, i.e.,

the ‘active’ and ‘passive’ interactions. Here, the ‘active’ interaction refers to SFT being driven to move so that it interacts with other defects such as grain boundaries (GBs), free surfaces and interfaces [14]. For the ‘passive’ interaction, however, SFT keeps still while other mobile defects move to interact with it [15,16].

Dislocation-SFT interaction, as an example of ‘passive’ defect-SFT interaction, is a more complex scenario than envisioned originally in which an SFT is simply absorbed and annihilated by the dislocation via a reversal of the Silcox-Hirsch formation process [17]. Three product defects are observed in experimental studies. They are the replacement of the SFT with a Frank loop [18–23], the SFT cancelled by dislocation with no residual defects left [23] and the replacement of the initial SFT with a smaller one [19–23]. Furthermore, the dislocation-SFT interactions revealed by molecular dynamic (MD) simulations include: the shearing of the SFT followed by its complete restoration [24–28], the SFT partially absorbed by the dislocation, leaving behind a smaller SFT [27,28] and partial or complete absorption of a truncated SFT by the dislocation [29,30].

We recently showed that the presence of an SFT near Cu coherent twin boundary (CTB) not only leads to the smaller yield stress of CTB bicrystal under shear, but also produces two CTBs. In addition, SFT may flip over when the CTB migrates during the shear loading [31]. The SFT flip-over is attributed to the local hydrostatic

\* Corresponding authors.

E-mail addresses: [wenshan@mail.xjtu.edu.cn](mailto:wenshan@mail.xjtu.edu.cn) (W. Yu), [sshen@mail.xjtu.edu.cn](mailto:sshen@mail.xjtu.edu.cn) (S. Shen).

compressive stress resulting from CTB migration. However, how the presence of an SFT near GB influence the shear properties of GBs with other misorientations still remains unknown.

This work focuses on the analysis of the interaction between an SFT and Cu GBs under shear. To this end, MD simulations are performed on four different copper symmetric tilt GBs, i.e.,  $\Sigma 9$ -(114),  $\Sigma 9$ -(221),  $\Sigma 11$ -(113) and  $\Sigma 11$ -(332), containing an SFT of three different sizes. The main reason why we select these four GBs in this study is that GBs with misorientations of  $\Sigma 9$  and  $\Sigma 11$  are usually observed in the polycrystalline materials and GBs tend to have GB plane with smaller indexes in realistic materials [32]. The influence of SFT on the shear properties of GBs are studied. We also analyze the atomistic structures involved in the GB deformations and SFT configuration evolutions during the shear.

## 2. Methodology

Fig. 1 schematically shows a Cu bicrystal model with an SFT placed in the vicinal GB. The GB models are setup by constructing two separate crystals (grains A and B) and joining them along the y direction. The tilt axis [1 1 0] is parallel with the x direction while GB normal direction is along the y direction. An SFT in the vicinity of GB can be created by removing specified numbers of vacancies  $N$  ( $N = n(n+1)/2$  ( $n > 2$ )) within a triangular region on the  $(\bar{1}11)$  plane [17]. Three different SFT sizes are considered, i.e., 10, 21 and 36 vacancies denoted as 10 V, 21 V and 36 V respectively.

The dimensions and geometrical parameters of the four symmetric GB models are listed in Table 1. Periodic boundary conditions are applied in the x and z directions while the top and bottom surfaces of the model are traction free. To obtain the GB structure with lowest energy for the further investigations, all as-constructed GBs are optimized by using Tschopp et al.'s approach [33–35], i.e., removing excess atoms in them and performing rigid body translations (RBTs). This yields average energies of four optimized GBs in agreement with the results from Ref. [33], as shown in Table 1.

All MD simulations in this study are performed using NVT ensemble with Nosé–Hoover thermostat at 300 K, using the

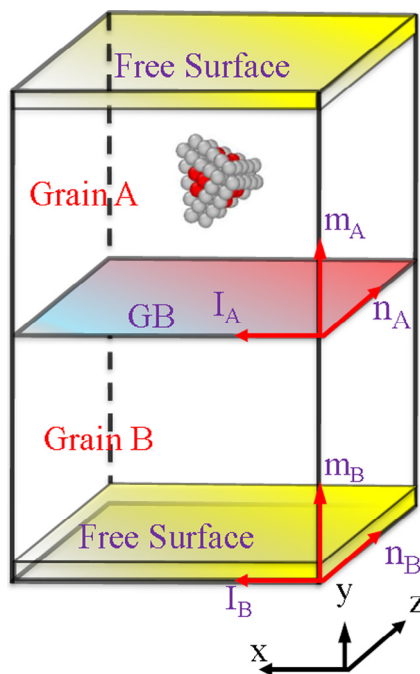


Fig. 1. Schematic of Cu bicrystal model with an SFT placed in the vicinal GB.

Table 1

The geometrical and physical properties of four GBs.

GBs	Model size $L_x \times L_y \times L_z/\text{\AA}^3$	GB energy/ ( $\text{J m}^{-2}$ )	GB energy/ ( $\text{J m}^{-2}$ )
$\Sigma 9$ -(114)	$61.2 \times 337.4 \times 65.1$	0.633	0.623
$\Sigma 9$ -(221)	$61.2 \times 325.4 \times 61.3$	0.814	0.833
$\Sigma 11$ -(113)	$61.2 \times 335.70 \times 67.8$	0.295	0.308
$\Sigma 11$ -(332)	$61.2 \times 339.12 \times 70.8$	0.695	0.704

<sup>†</sup> Present results.

<sup>\*</sup> Results taken from Ref. [33].

software LAMMPS [36] with the embedded-atom-method potential for Cu developed by Mishin et al. [37]. Homogeneous shear loading is achieved by displacing the top 10 Å thick slab in the z direction while the bottom slab fixed. The shear strain step and strain rate are  $3 \times 10^{-5}$  and  $10^8 \text{ s}^{-1}$ , respectively. Microstructures and deformation mechanisms are analyzed using common neighbor analysis (CNA) method [38,39] in the software OVITO [40].

## 3. Results

### 3.1. The shear response

Considering the shear response of the four GBs in perfect GB bicrystal have been well studied [41–44], we only briefly introduce the transformation mechanism of SFT and the influence of SFT on the mechanical behavior of the four GBs under shear. Besides, we also study the shear response of the  $\Sigma 11$ -(332) GB bicrystal with an SFT loading in the tilt-axis direction (x-direction) to investigate the transformation mechanism of SFT in the condition of GB sliding mode, and its stress-strain curve is shown in Fig. S1 in Supplementary Materials.

The shear response of GB bicrystals with an SFT (10 V, 21 V and 36 V) loading in the z direction are shown in Fig. 2. The stress-strain curve of a perfect GB bicrystal is plotted as well for comparison. It can be seen that the GB bicrystals with an SFT has a stress response similar to that of the perfect GB bicrystal, i.e. most of these stress-strain curves exhibiting the saw-tooth profile. Each sudden drop in stress corresponds to a particular plastic deformation event to release the local stress concentration in GB bicrystal, for example the migration and dissociation of GB, the nucleation of partial dislocations from the GBs, the interactions between SFT with partial dislocations and between SFT with GBs. From Fig. 2, the presence of an SFT influences the shear response of a bicrystal in two aspects. One, evidenced by the first drop of stress, is an effect on the critical stress related to the incipient plastic deformation. The SFT size indeed affects the critical stress of GB bicrystals, but such influence is not effective as shown by less than 0.4 GPa variation of critical stress for different SFT sizes in Fig. 9. Two is the difference between stress-strain curves after incipient plasticity. These are mainly due to the presence of SFT and the different underlying transformation mechanisms of SFT.

### 3.2. The transformation of SFTs in the $\Sigma 9$ -(114) and $\Sigma 9$ -(221) GB bicrystals

Some snapshots of the  $\Sigma 9$ -(114) and  $\Sigma 9$ -(221) GB bicrystals with an SFT in the plastic deformation stage are shown in Fig. 3. Only are snapshots for 36 V SFT in the  $\Sigma 9$ -(221) GB bicrystal shown in Fig. 3. Results for 10 V and 21 V SFT, similar to that of 36 V SFT are given in Fig. S2 in Supplementary Materials. In Fig. 3, we can see that the partial dislocations are emitted from GB, the highly disordered GB structures are produced due to atom-shuffling and the partial dislocations interact with SFT. For

Download English Version:

<https://daneshyari.com/en/article/7957756>

Download Persian Version:

<https://daneshyari.com/article/7957756>

[Daneshyari.com](https://daneshyari.com)